applied sciences

MDPI

Article

Design and Simulation Study of Structural Parameters of Bionic Cutters for Tea Harvest Imitating *Aeolesthes induta* Newman

Yuanqiang Luo, Junlin Li, Song He and Weibin Wu *

College of Engineering, South China Agricultural University, Guangzhou 510642, China; luoyq@scau.edu.cn (Y.L.); ljldragonquest@stu.scau.edu.cn (J.L.); songhe@stu.scau.edu.cn (S.H.)
* Correspondence: wuweibin@scau.edu.cn

Abstract: The cutter of the hand-held tea picker is the key cutting component in the efficient tea harvesting process. In order to solve the problems of large cutting resistance and uneven incision during tea picking, this study fully applied the bionics principle to combine the excellent cutting performance of *Aeolesthes induta* Newman's mandibles with the tea cutter, which extracted and fitted the tooth profile structure curve of the upper edge of the *Aeolesthes induta* Newman's mandibles. The trapezoidal teeth on the reciprocating cutter of ordinary hand-held tea-picking harvesters were optimized by the fitted curve, and a new tea cutter with the shape of *Aeolesthes induta* Newman teeth was obtained, which included four kinds of bionic tea-harvesting cutters. The multi-body system software ADAMS 2020 and finite element analysis software ANSYS 2024R1 were used to compare the kinematics, statics and explicit dynamics of cutting properties of the four bionic cutters and common cutters with ordinary trapezoidal teeth and saw teeth. The simulation results showed that the maximum equivalent elastic strain and the maximum cutting force during the cutting operation were reduced by 36.7% and 42.89%, respectively, for the cutting teeth of the bionic tea-harvesting cutter #4 compared with that of the cutter with ordinary trapezoidal teeth. The bionic tea-harvesting cutter designed in this study has better cutting performance than the cutter with traditional cutting teeth, which can effectively reduce the cutting force and improve the flatness and cutting quality of the cutting surface.

Keywords: bionic harvesting; cutting type end-effector; agricultural biomimicry; *Aeolesthes induta* Newman

check for updates

Citation: Luo, Y.; Li, J.; He, S.; Wu, W. Design and Simulation Study of Structural Parameters of Bionic Cutters for Tea Harvest Imitating *Aeolesthes induta* Newman. *Appl. Sci.* **2024**, *14*, 9763. https://doi.org/10.3390/app14219763

Academic Editors: Ana Martins Amaro and Alessandro Lo Schiavo

Received: 16 July 2024
Revised: 4 September 2024
Accepted: 15 October 2024
Published: 25 October 2024

Copyright: © 2024 by the authors. Licensee MDPI, Basel, Switzerland. This article is an open access article distributed under the terms and conditions of the Creative Commons Attribution (CC BY) license (https://creativecommons.org/licenses/by/4.0/).

1. Introduction

In the 21st century, tea, a healthy drink, has become more popular in countries around the world [1]. China is the world's largest tea producing country and tea consumption market [2]. However, with the acceleration of global population aging, there is a shortage of tea farmers' labor and resulting low efficiency. At the same time, tea harvesting is the most time-consuming work in tea making. Therefore, it is necessary to improve the mechanization level of tea harvesting. For a long time, the relevant research of machine harvesting tea has been carried out at home and abroad. For the study of excellent tea, a number of scholars introduced the research scheme of "hand-picking" (manual picking action of fixing and lifting tea leaves [3]) in the tea picking machine. Hao et al. [4] proposed an electrically driven picking finger prototype based on the mechanics and morphological characteristics of new green tea tips. Based on this, Liu et al. [5] further completed the picking finger drive control system hardware circuit design and software development, and the experimental results show that the picking finger can effectively separate the tea leaves from their stalks, achieving a bud- and leaf-picking success rate of 90%. Even at present, the sophisticated tea picking machine has been widely developed but still cannot be widely used; the reason is that the majority of poor tea farmers cannot afford its expensive cost.

In recent years, more and more scholars have applied the concept of bionics, the power of nature, to various fields, and the number of related research results has been rising [6,7],

which will certainly bring a new round of technological innovation in the future [8]. In this context, the agricultural harvesting field has taken advantage of the trend to deal with the lack of labor and to alleviate harvesting costs for poor tea farmers through the use of bionics technology. "What's taken from the agro-biology is used for the agro-biology", is a better choice for future agricultural development [9].

At present, bionics technology that improves the cutting performance of tools with the help of the power of nature has become a popular research topic in the agricultural field [10–12]. In a study by Tian et al. [13–15], based on the excellent cutting characteristics of batocera horsfieldi's upper jaw teeth on the hard stems of plants, a bionic picking and cutter with more level stubble and lower resistance and energy consumption was designed to cut cannabis stalks. Tang et al. [16] designed a bionic single-disc top cutting device for harvesting carrots based on the forelimb structure of mantises. In addition, Liu et al. [17] extracted the contours of the upper incisor flap of crickets and designed a bionic cutting blade for picking wild chrysanthemums. The power consumption of the cutting machine equipped with the bionic cutting blade could be reduced by 10.80%. Jia et al. [11] designed a bionic cornstalk cutting blade inspired by grasshopper serrated incisor-cutting plant fibers, whose average cutting force was 28.17% lower than that of traditional blades, and cutting energy consumption was 12.85% lower. In conclusion, it is not difficult to see that most of the above scholars carried out bionic optimization designs of the outline structures of cutting tools by imitating the sharp structures of the insects, which effectively reduces the cutting resistance and cutting energy consumption of the cutting tool.

Therefore, this study introduces bionics technology into the hand-held reciprocating cutting tea-harvesting machine, which is widely used because of its cheap and easy operation, so as to improve the mechanization of tea harvesting and solve the problems of labor shortage and low efficiency of tea farmers [18,19]. As the main component of a tea harvesting-machine, the structure of the tea cutter has a crucial impact on cutting resistance, cutting power consumption and quality during tea harvesting [20,21].

However, due to the fact that most tea picking machines in China are designed to imitate Japanese machines, the parameters of tea cutters are also directly designed to imitate [22], and the tooth shape of conventional trapezoid teeth is not further optimized. Due to the limitations of the structure itself, there is still a lot of room for improvement in harvesting quality.

For more than 3000 years, nature has been acting as the mentor of human beings, and the excellent characteristics of biology have inspired human designs. Therefore, in this study, the mechanism of tea tree stem cutting by *Aeolesthes induta* Newman when feeding on tea was studied, and the cutter structure of tea picker was further optimized based on bionics principles so as to improve the performance and quality of tea cutting. The rest of this paper is organized as follows: Section 2 introduces the process and extraction of the fitting curve of the *Aeolesthes induta* Newman sample in this study. Section 3 analyzes the bionic design and simulation of tea cutters and compares and analyzes the results. Section 4 presents a discussion of the work. Section 5 introduces the limitations and future directions of this study.

2. Materials and Methods

2.1. Aeolesthes induta Newman

Aeolesthes induta Newman is a common tea tree pest in domestic tea gardens, which belongs to *Coleoptera*, *Cerambycidae*, and is also known as neem aspen, tea brown aspen and heartworm. *Aeolesthes induta* Newman is one of the tea tree boring pests [23] whose larvae or adults feed on the tea tree branches, causing damage, poor growth of the affected tea trees and even death, as shown in Figure 1. In the context of natural selection, the *Aeolesthes induta* Newman evolved a chewing mouthpiece that can be used to chew food, dig holes, build nests and hunt enemies. The upper jaw of the *Aeolesthes induta* Newman's mouthparts is a pair of curved mandibles divided into incisors and molar lobes. The incisor lobe is the curved portion of the tip of the upper jaw that is primarily used for piercing

and tearing food, while the root structure of the teeth is known as the molar lobe and is primarily used for chewing and grinding food.

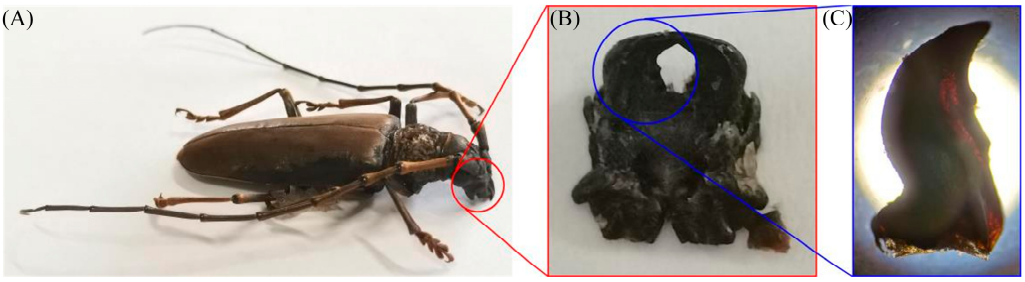


Figure 1. *Aeolesthes induta* Newman. (**A**) Sample; (**B**) The upper part of the mouth; (**C**) Single-curved tooth structure.

The *Aeolesthes induta* Newman benefits from the curved structure of the upper mouth of its mouthparts, which makes it easy to cut and tear the tea stalk fibers during its daily foraging in tea gardens. It is the curved structural characteristics of the upper jaw mouthpiece of the *Aeolesthes induta* Newman that reduces drag and energy consumption as well as improves the quality of the cutting teeth and the cutter's harvest. Based on the mandibles used by tea pests (*Aeolesthes induta* Newman) for cutting tea stems, this study carried out bionic design of tea-harvesting cutters also used for cutting tea stems, which is in line with the bionic agricultural concept of "What's taken from the agro-biology is used for the agro-biology" [9].

2.2. Sample Processing

Based on bionics theory, by extracting the outer contour curve of the mandibles of the *Aeolesthes induta* Newman, the cutting teeth of the cutter are designed and machined with a similar curved contour structure to achieve an efficient cutting effect. After the *Aeolesthes induta* Newman captured from Yinghong Town, Yingde City, Guangdong Province, China (113.45 N, 24.37 E), died naturally (Figure 1A), the mouthparts of the *Aeolesthes induta* Newman were separated from their heads with a medical scalpel (Figure 1B), washed in distilled water and air-dried. Since the adult tea beetle is relatively hidden in the tea tree, an adult tea beetle was obtained as the experimental sample after a long period of trapping.

In order to clearly and accurately extract the parameters of the edge profile curve of the mouthparts, the prepared samples of the maxillary mouthparts of the *Aeolesthes induta* Newman were observed under the objective lens of a biological microscope (ML31, Mshot, China), and the focus of the microscope's objective lens was adjusted until the curved, single-toothed structure of the *Aeolesthes induta* Newman was clearly visible on the computer display (Figure 1C), and photographs of the structures were taken and stored using the software that was provided with the microscope.

2.3. Extraction and Analysis of Maxillary Contour Curve

After obtaining the contour structural images of the maxillary mouthpart samples of *Aeolesthes induta* Newman from the bio-microscope, as shown in Figure 2, the images were pre-processed by grayscaling and binarization in this study. The MATLAB embedding commands "rgb2gray", "imbinarize", "logical", "im2uint8" and "imcomplement" were used to ensure that the edges of the complete maxillary mouthparts were clearly segmented (Figure 2B–D), and the smooth function in MATLAB was then used to ensure robustness to noise cancellation and passive edges in the original image in order to reduce errors in image edge detection (Figure 2E). Then we used the bwboundaries function to extract the outer boundary information of the maxillary mouthparts contour and used the plot function to draw them into a two-dimensional line graph to complete the edge extraction of the mouthparts of the *Aeolesthes induta* Newman, and finally, to establish the contour curve

with a clear and complete line, which is consistent with the outer contour of the curvature of the *Aeolesthes induta* Newman's mouthparts (Figure 2F).

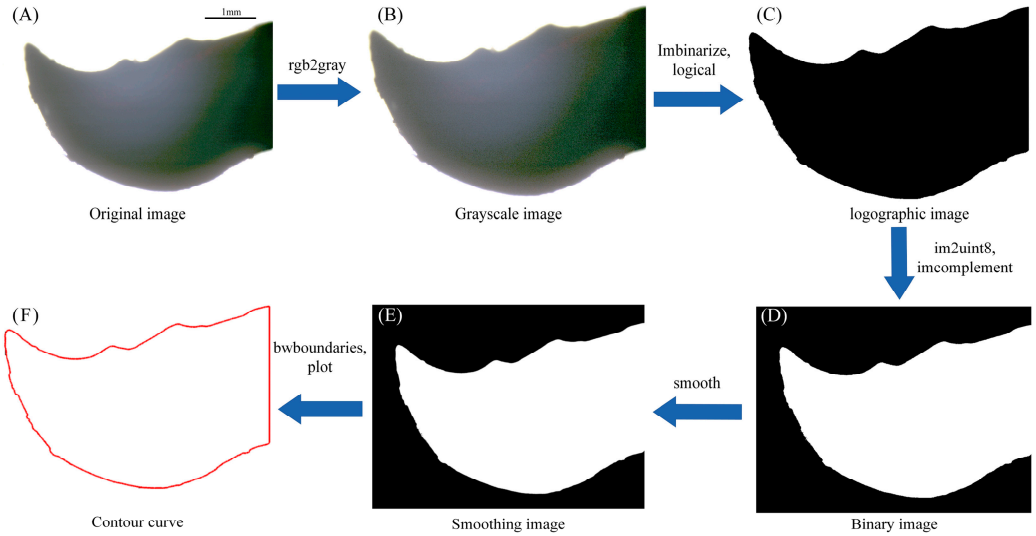


Figure 2. *Aeolesthes induta* Newman and its mouthpiece structure.

In this study, the coordinates of the extracted boundary points are plotted to extract the polynomial equation of the maxillary profile to simplify the shape of the tooth. In the fitted curves, the value of the correction coefficient of determination, $Adj.R^2$, is used as an optimal indicator in the search for the best fitting matching equation. In Figure 3, O is the origin of the reference coordinate system, and we establish the Cartesian coordinate system XOY on the two-dimensional plane. In order to optimize the contour structure of the tea cutter edge, we only analyzed the outer edge curve of the maxillary structure that plays a cutting role and divided the maxillary contour of the mouth into three curves to express the contour curve more accurately.

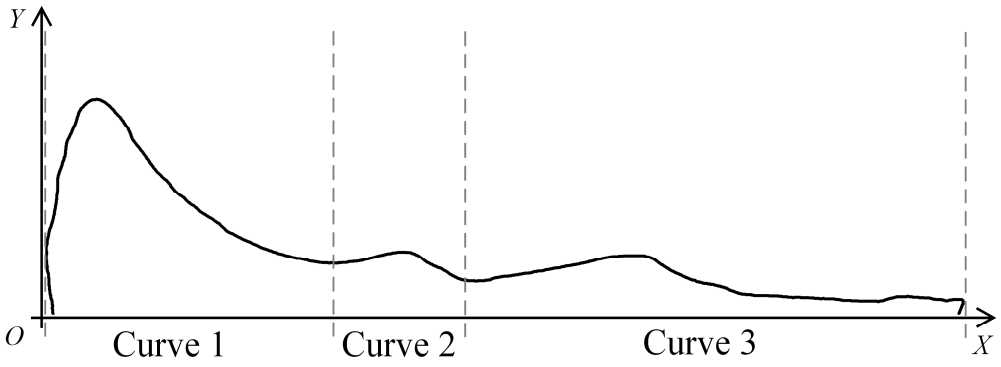


Figure 3. Extracted contour line of the teeth of the *Aeolesthes induta* Newman.

In order to improve the fitting effect and bionic degree, this study used the Levenbers Marquardt optimization algorithm of ORIGIN's nonlinear regression model to fit the maxillary contour curves of three mouthparts respectively, and expressed them with a quintic polynomial function, as shown in Equation (1).

$$y(x) = a_0 + a_1x + a_2x^2 + a_3x^3 + a_4x^4 + a_5x^5 \quad (1)$$

The fitting parameters of the structure curve of the outer edge of the palate are shown in Table 1. From Table 1, it is found that the $Adj.R^2$ of all the curves (curvel 1, curvel 2 and curvel 3) is greater than 0.962; therefore, it is proved that the treatment presents a high degree of fit.

Table 1. Parameters of the fitted curves.

Parameters	Curvel 1	Curvel 2	Curvel 3
a_0	−412.141	−47,254.389	12,169.170
a_1	23.791	819.915	−117.612
a_2	−0.330	−5.634	0.445
a_3	0.0021	0.019	-8.226×10^{-4}
a_4	-6.096×10^{-6}	-3.234×10^{-5}	7.421×10^{-7}
a_5	7.004×10^{-9}	2.161×10^{-8}	-2.621×10^{-10}
$Adj.R^2$	0.994	0.992	0.962

Three fitted curves have upward and downward trends, as shown in Figure 4A. The peak value of curve 1 is the highest, which is much higher than the maximum value of other curves, while curve 2 and curve 3 only rise a little and then decrease.

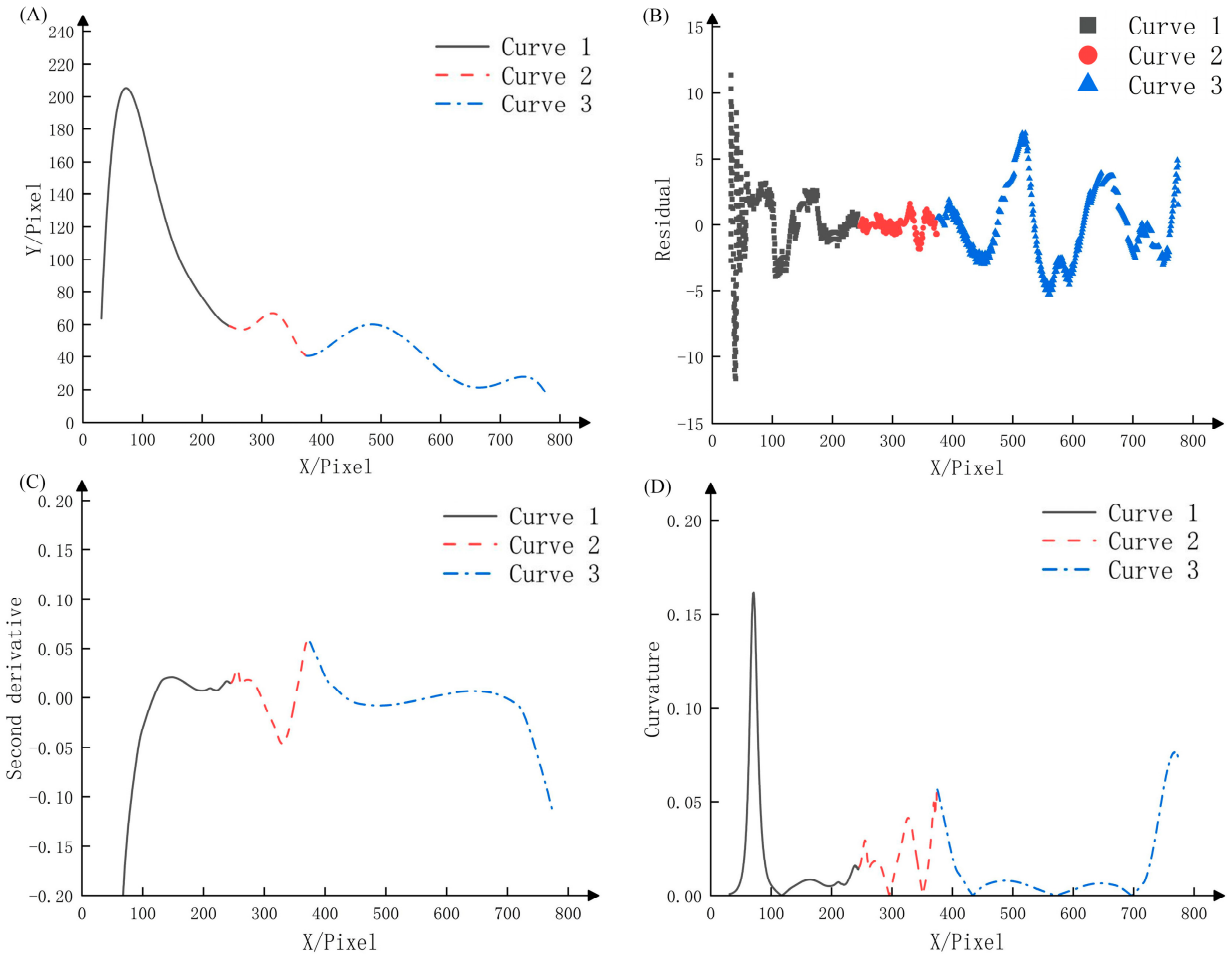


Figure 4. Fitted curve of upper jaw and its residual value. (**A**) Fitted curve; (**B**) Residuals; (**C**) Second derivative; (**D**) Curvature.

Figure 4B shows the residuals after fitting curves. The absolute values of residuals on all curves are within or near ±10. The lower the absolute value of residuals, the higher the degree of fitting. Then the second derivative functions of 3 fitted curves were obtained, and the graph analysis diagram was drawn (Figure 4C). The second derivative function can reflect the concavity of the contour of the upper mouth of the original image. When the second derivative function is less than 0, it proves that the inner curve in this area shows the property of convex function. It is not difficult to see that the shapes of curves 1–3 all protrude outwards, which can increase the contact pressure between the external contour

of the maxillary mouthparts and the material in the cutting process, where the second derivative value of curve 1 rises from −0.500 to 0.021 and then drops to about 0.007. The minimum value of the second derivative of curve 1 is smaller than those of curve 2 and curve 3, indicating that curve 1 is more convex.

The sharpness of the contour structure of the inner edge of the maxillary incisor lobes plays a key role in the feeding process of *Aeolesthes induta* Newman. It is obvious from Figure 4D that the curvature value of curve 1 is much greater than other curves, indicating that curve 1 has greater curvature than curve 2 and curve 3, and the corresponding incisor lobe is sharper, which is conducive to cutting the stem of tea. Among them, the fitting equation of curve 1 is shown in Equation (2).

$$y(x) = -412.1416 + 23.791x - 0.330x^2 + 0.0021x^3 - 6.096 \times 10^{-6}x^4 + 7.004 \times 10^{-9}x^5 \quad (2)$$

3. Design and Simulation of Bionic Tea Cutters

3.1. Design of the Bionic Cutters

In order to achieve the goal of reducing cutting resistance of the tool and smooth cutting of the stalk, this study is based on the basic structural parameters and relevant size parameters of the tea cutter commonly available in the market and ensures that the working capacity of the portable tea-harvesting machine meets the production requirements. Therefore, the basic data of the four schemes of bionic tea cutters are set as follows: The total length of cutter l is 310 mm, cutter thickness i is 1.1 mm, the cutting tooth height of cutter h is 30 mm, the tooth thickness of cutter s is 30 mm, the space width of cutter t is 10 mm. Each cutter has 10 cutting teeth.

Based on the above dimensions, this study took the fitting curve of the maxillary tooth profile of the mouth parts of the *Aeolesthes induta* Newman as the contour structure curve of the cutting tooth profile of the cutter so as to carry out bionic optimization design of the tea cutter and establish a three-dimensional model of the bionic tea-harvesting cutter, as shown in Figure 5.

Each scheme of bionic tea-harvesting cutters is different and has its own characteristics. Among them, the teeth of in bionic tea-harvesting cutter scheme 1 are distributed along the handle, the tip points are consistent and the two cutters are assembled with the tip relative to each other, as shown in Figure 5A. The structure of bionic tea-harvesting cutter #2 is roughly the same as that of bionic tea-harvesting cutter #1. The difference is that in the multi-cutting teeth of the same cutter, the tip of the adjacent two cutting teeth face opposite directions, as shown in Figure 5B. In addition, the bionic tea-harvesting cutters #1 and #2 have the same structural size of cutting tooth used, named bionic cutting tooth 1.

In order to further improve the bionic optimization application degree of the tooth profile fitting curve of the upper jaw of the *Aeolesthes induta* Newman on the tea-harvesting cutters, based on the first two schemes, the cutting tooth contour curve of bionic tea-harvesting cutter #3 is symmetrically set on both sides of the cutting teeth. In addition, the cutting tooth design of bionic tea-harvesting cutter #3 is named bionic cutting tooth 2, as shown in Figure 5C.

From Section 2, it can be seen that the incisor lobe of the maxillary mouthparts of *Aeolesthes induta* Newman mainly plays the role of piercing and tearing food. In this study, it is curve 1, whose curvature is $Adj.R^2$. Therefore, in order to improve the cutting and tearing ability of tea cutters on tea stems, in this study, curve 1 was selected to model the saw tooth of the cutter so as to design the cutting tooth of the bionic tea-harvesting cutter #4, which only consists of curve 1. The cutting tooth design of the bionic tea-harvesting cutter #4 is based on the ordinary trapezoid tooth, and only curve 1 is used to carry out the bionic design of the tooth outline structure on both sides of the ordinary trapezoid cutter tooth edge. In addition, the cutting tooth of bionic tea-harvesting cutter #4 is named as bionic cutting tooth 3, as shown in Figure 5D.

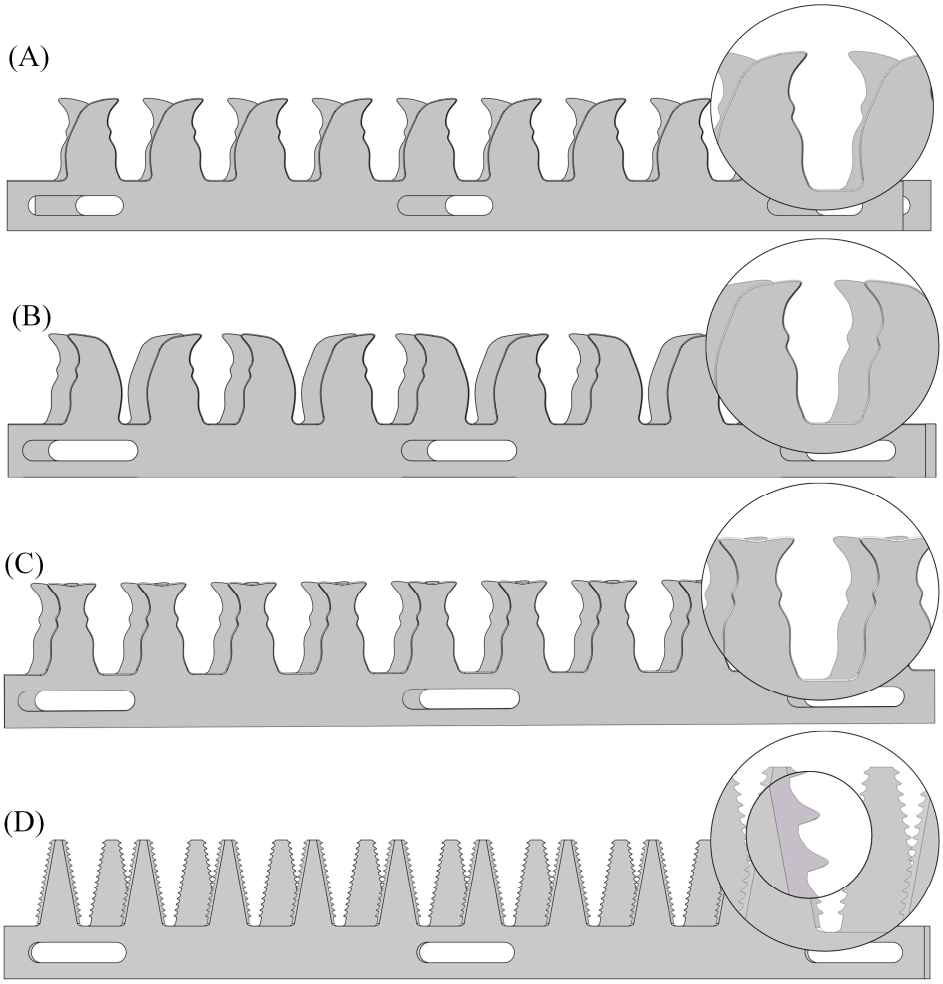


Figure 5. Three-dimensional model of four cutter schemes. (**A**) Bionic tea-harvesting cutter #1; (**B**) Bionic tea-harvesting cutter #2; (**C**) Bionic tea-harvesting cutter #3; (**D**) Bionic tea-harvesting cutter #4.

3.2. Kinematics Analysis

In this study, after the preliminary analysis of the reciprocating cutting motion of the four schemes of bionic tea cutters, it is not difficult to find that the cutting teeth of bionic cutter #1 and #2 are bionic cutting teeth 1 and have three kinds of cutting collocation modes, that is, the bionic cutting teeth 1 of the two cutters are relative to each other (Figure 6A), bionic cutting teeth 1 tip in the same direction (Figure 6B) and bionic cutting teeth tip opposite (Figure 6C). In addition, the bionic cutting teeth 2 and the bionic cutting teeth 3 represented by the bionic cutter #3 and #4 respectively have only one cutting collocation mode (Figure 6D,E).

It is not difficult to find from Figure 6 that tea stems in the first three bionic cutter schemes are not completely cut by curve 1 fitted by the incisor lobe, or even mostly cut by curve 2 and curve 3. Secondly, among the three cutting modes produced by bionic tea-harvesting cutters #1 and #2, only cutting collocation mode I is cutting with the relative motion of the bionic fitting curve. It is obvious that cutting collocation mode III produced by bionic cutters #1 and #2 (Figure 6C) is the result of the tea stem being located between the outer convex arc outline structure of two bionic cutting teeth. Therefore, the cutting collocation mode III is prone to the phenomenon of insufficient cutting in the actual cutting of tea stems, so it is necessary to further carry out the kinematics simulation analysis of the bionic tea-harvesting cutter scheme.

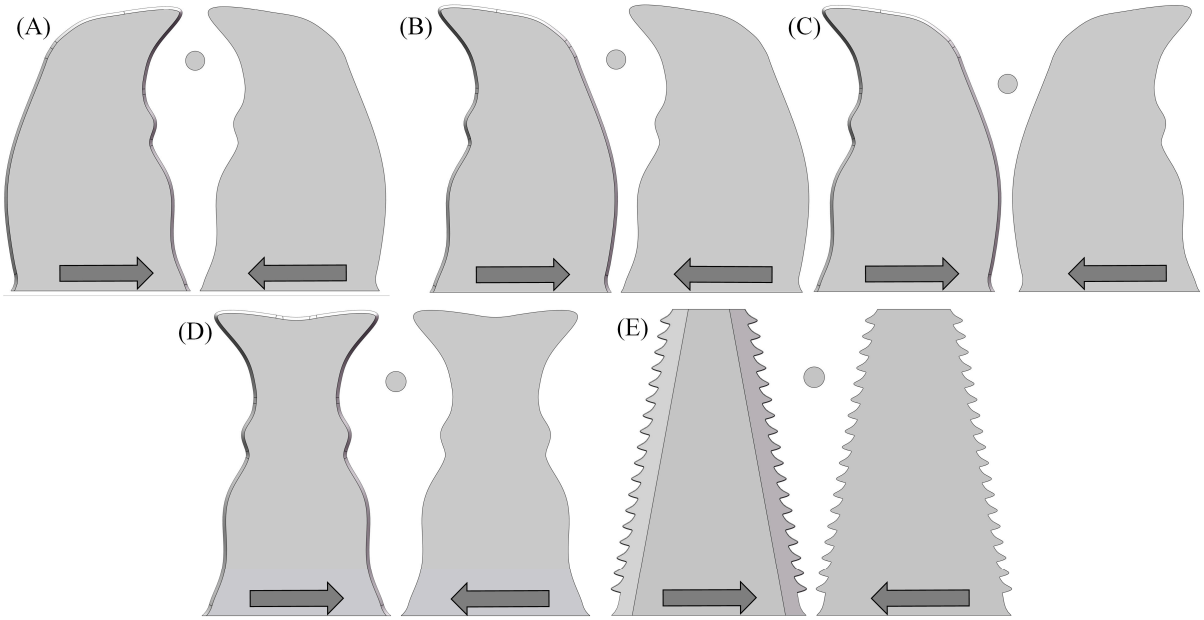


Figure 6. The cutting teeth of the four schemes cut the tea stalk (the gray circle represents the tea stalk, and the gray arrow represents the movement direction of the bionic cutting teeth). (**A**) Cutting collocation mode I of bionic cutting teeth 1; (**B**) Cutting collocation mode II of bionic cutting teeth 1; (**C**) Cutting collocation mode III of bionic cutting teeth 1; (**D**) Cutting collocation mode of bionic cutting teeth 2; (**E**) Cutting collocation mode of bionic cutting teeth 3.

In this study, the 3D structural model of the bionic tea-harvesting cutter was further imported into ADAMS and constraints and drivers were added to build a kinematic model of the bionic tea-harvesting cutter build for testing. It is obvious from Figure 6E that the tooth shapes of bionic tea-harvesting cutter #4 are all designed based on the curve 1, that is, bionic tea-harvesting cutter #4 mainly relies on the outline structure designed by the curve 1 for cutting operations. Therefore, in this section, only the first three scenarios of the bionic tea-harvesting cutter are specifically simulated and analyzed, and the specific operations are as follows.

In this study, the two bionic tea-harvesting cutters are set to move forward as a whole, and the virtual motor drives the cam mechanism to make one of the cutters reciprocate, which is set to be a moving cutter, and the other cutter only moves forward and is stationary with respect to the virtual motor-driven cutter, which is a fixed cutter, as shown in Figure 7. A MARK point is established at the end of the lowest depression of curve 1 of the bionic tea-harvesting cutter, and the motion trajectory of the MARK point is obtained. The intersection of the end points at the lowest depression of curve 1 of the two bionic tea-harvesting cutters is a complete cutting process, and the motion cutting trajectory diagram of the two bionic tea-harvesting cutters is formed. As shown in Figure 7, point a is the MARK point on the fixed cutter, and point b and point c are the MARK points on the moving cutter.

From Figure 7, it can be seen that the first two schemes made only one cut in curve 1 in one cutting cycle, while #3 made two cuts in one cutting cycle, which proves that #3 relies more prominently on the bionic contour for the cutting operation than the first two bionic schemes. Similarly, the bionic tea-harvesting cutter #4, composed only of curve 1, can better highlight the harvesting operation carried out by the bionic structure.

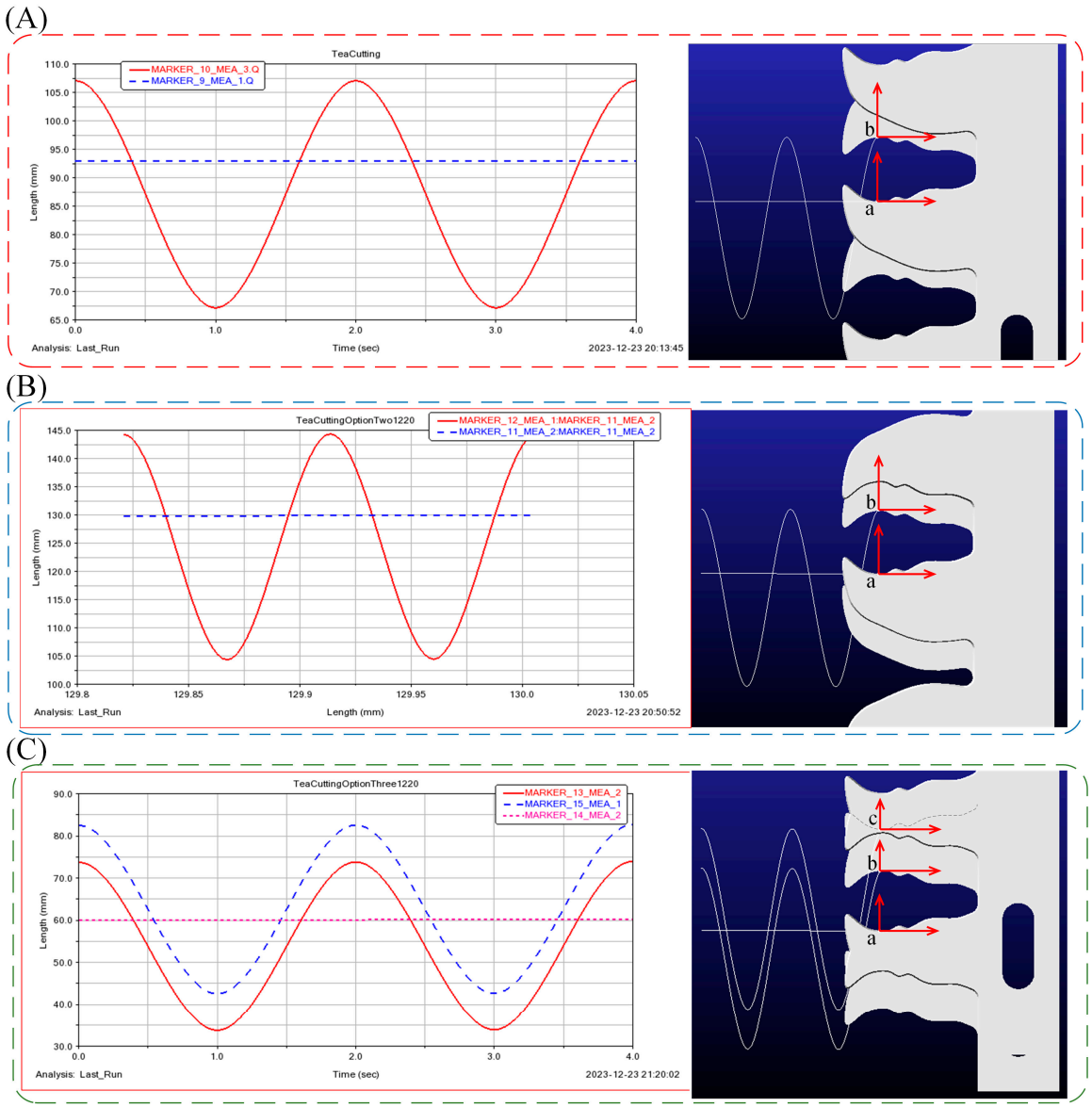


Figure 7. Motion cutting trajectory diagram of bionic tea-harvesting cutters. (**A**) Bionic tea-harvesting cutter #1; (**B**) Bionic tea-harvesting cutter #2; (**C**) Bionic tea-harvesting cutter #3.

3.3. Statics Analysis

Among the four bionic tea-harvesting cutter schemes, there are three kinds of bionic cutting tooth-shape structures with different shapes, as shown in Figure 6. In view of the impact of the interaction between bionic tea-harvesting cutter and stalk on the cutting tooth, the static simulation analysis of the three kinds of bionic tooth-shape structures is carried out, and the comparison is made with the ordinary trapezoid tooth and the ordinary saw tooth of cutter. The detailed operations are as follows.

The 3D cutting tooth models of four bionic tea-harvesting cutter schemes were imported into the Static Structural of ANSYS workbench in STP format, and the cutting tooth material was set as Structural Steel in Engineering Data. Secondly, Mesh is selected to refine the surface of the cutting tooth edge of the bionic tea-harvesting cutter. Since the bionic cutting tooth and the tea-harvesting cutter structure are integrated, that is, static relative to the cutter, a fixed support constraint is added to the bottom of the bionic cutting tooth, and 3N resistance is assumed on the edge surface of the left and right sides of the bionic cutting tooth, applied in opposite directions, as shown in Figure 8.

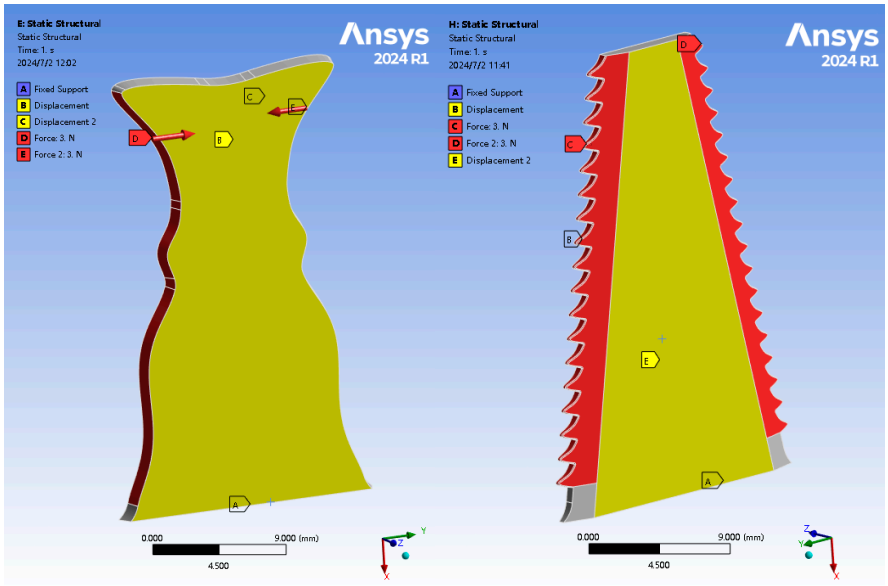


Figure 8. Static structural constraint load settings for bionic cutting teeth 3 and 4.

Figure 9 shows the total deformation cloud map of common trapezoid teeth, the saw tooth and three bionic cutting teeth. The red part is the part with large total deformation. It can be clearly seen that this part is the contact position between the bionic cutting tooth and the tea stalk, that is, the cutting edge of the bionic cutting tooth. The total deformation gradually increases from the root part to the cutting tooth edge part, and the total deformation of the middle part of the cutting tooth is smaller than that of the horizontal sides.

From Table 2, it can be seen that the maximum equivalent force values of bionic cutting tooth 1, bionic cutting tooth 2 and bionic cutting tooth 3 have been reduced by 78.07%, 81.28% and 81.83%, respectively, with respect to the maximum equivalent force values of normal trapezoidal teeth. It is clearly seen that the maximum equivalent force value of the bionic cutting tooth 3 is much lower than that of the normal trapezoidal tooth, and lower than that of the bionic cutting tooth 1 and the bionic cutting tooth 2. Compared with the maximum equivalent force value of ordinary saw tooth, the bionic cutting tooth 3 reduces by 29.54%. The smaller the maximum equivalent force value, the less stress concentration phenomenon, which proves that the bionic cutting tooth 3 is less prone to fracture failure in the actual cutting operation.

Table 2. Static simulation data results.

Cutting Tooth	Maximum Equivalent Stress/MPa	Maximum Equivalent Elastic Strain	Maximum Total Deformation/mm
Ordinary trapezoidal tooth	1.090	5.527×10^{-6}	8.805×10^{-6}
Bionic cutting tooth 1	0.239	1.194×10^{-6}	7.048×10^{-6}
Bionic cutting tooth 2	0.204	1.024×10^{-6}	5.796×10^{-6}
Ordinary saw tooth	0.281	1.405×10^{-6}	5.207×10^{-6}
Bionic cutting tooth 3	0.198	9.943×10^{-7}	4.853×10^{-6}

Compared with the maximum equivalent elastic strain value of ordinary trapezoidal teeth, the bionic cutting teeth 1, 2 and 3 decreased by 78.4%, 81.47% and 82.01%, respectively. It is obvious that the maximum equivalent elastic strain value of bionic cutting tooth 3 is much lower than that of the ordinary trapezoidal tooth, and lower than bionic cutting tooth 1 and bionic cutting tooth 2. Compared with the maximum equivalent elastic strain value of the ordinary saw tooth, the bionic cutting tooth 3 is reduced by 29.23%.

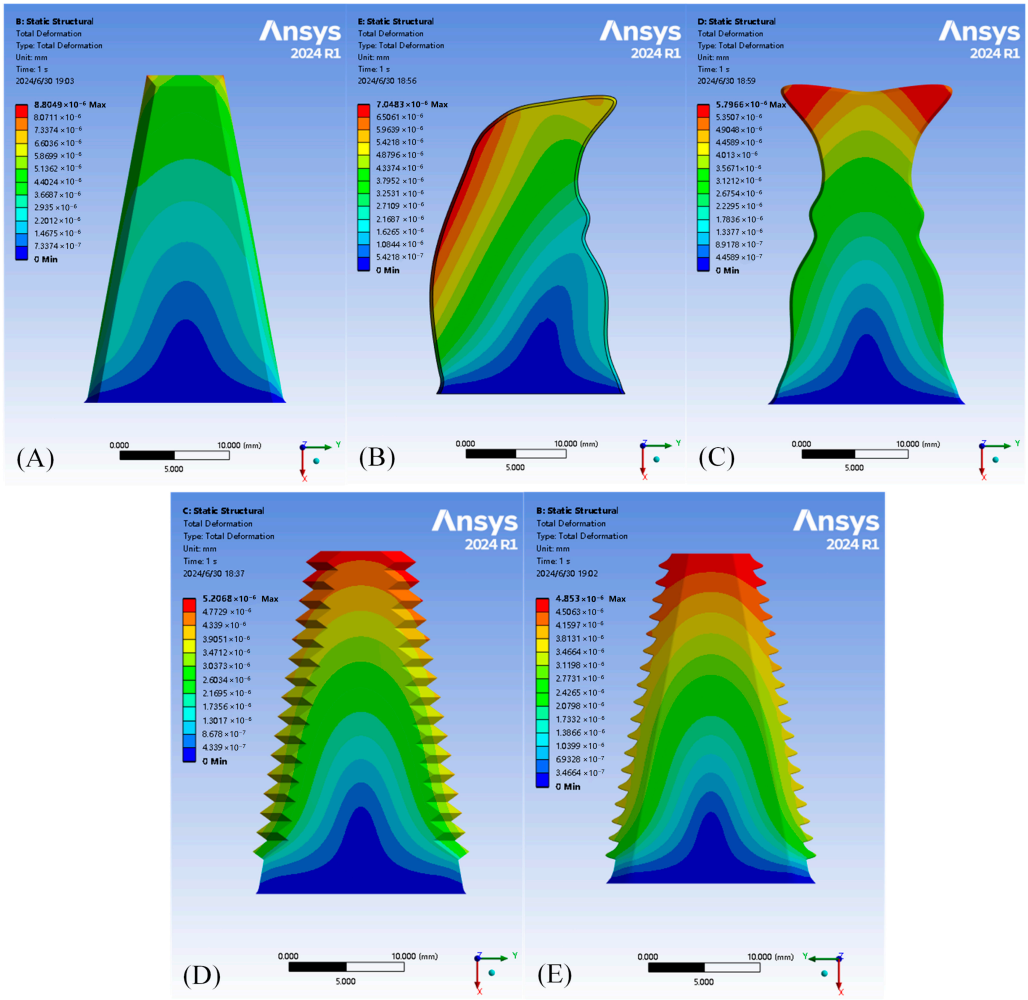


Figure 9. Static simulation test of cutting teeth. (**A**) Ordinary trapezoidal tooth. (**B**) Ordinary saw tooth. (**C**) Bionic cutting tooth 1. (**D**) Bionic cutting tooth 2. (**E**) Bionic cutting tooth 3.

Compared with the maximum total deformation of ordinary trapezoid tooth, the bionic cutting teeth 1, 2 and 3 are reduced by 19.95%, 34.17% and 44.88%, respectively. It is obvious that the maximum total deformation of bionic cutting tooth 3 is much lower than that of ordinary trapezoidal tooth, and lower than bionic cutting tooth 1 and bionic cutting tooth 2. The maximum total deformation of the bionic cutting tooth 3 is reduced by 6.80% relative to the maximum total deformation of the ordinary saw tooth. The smaller the maximum total deformation, the less likely the bionic cutting tooth 3 is to deform during actual cutting operations.

In summary, the maximum values of equivalent stress, equivalent elastic strain and total deformation of the bionic cutting tooth 3 are the smallest among all the cutting teeth under the same constraints and loads, proving that the bionic cutting tooth 3 represents the best cutting performance of the bionic tea-harvesting cutter scheme 4 in the practical application process.

3.4. Explicit Dynamic Analysis

In order to study the changes in the tea stalks during the harvesting of tea leaves by the cutter, the contact between the cutting teeth of bionic cutters and the stems was taken as the starting point and the stem breakage was taken as the end point. In this study, ANSYS Explicit Dynamics was used to conduct the explicit dynamic simulation test for the above work process. The detailed operations are as follows.

In this study, the bionic tea-harvesting cutter was set 70 mm away from the root of the tea stalk to cut the tea stalk. The 3D cutting tooth models of four bionic tea-harvesting cutter schemes are imported into the Explicit Dynamics of ANSYS workbench in STP format, and then the cutting teeth of the bionic tea-harvesting cutter and the cutting mechanical property parameters of tea stems are set in Engineering Data, as shown in Table 3. Secondly, material performance parameters and properties are specified for each model, with the stiffness of bionic cutting teeth as rigidity and the tea stalk as flexibility. We then use the Manual Contact Region in Connections and set the contact type as friction between the two bionic cutting teeth of each scheme and the tea stem, respectively, and the friction coefficient is 0.3. Finally, Mesh was selected to refine the surface of the cutting teeth edges and the whole tea stem module. The average diameter of the cross section of the tea stem was 2 mm.

Table 3. Parameters of cutting teeth and tea stalk.

Parameter Settings / Test Materials	Density/ kg·mm^{-3}	Isotropic Elasticity			
		Young's Modulus/MPa	Poisson's Ratio	Bulk Modulus/MPa	Shear Modulus/MPa
Cutting tooth	7.85×10^{-6}	200,000	0.3	1.6667×10^{5}	7.6923×10^{4}
Tea stalk	6×10^{-7}	54.28	0.344	57.991	20.193

In order to simulate tea harvest conditions, fixed support constraints were added to the lower part of the tea stem structure model (that is, the root of the tea stem), and Displacements were added to the two bionic cutting teeth to make the bionic cutting teeth produce horizontal relative displacements, thus realizing the cutting simulation analysis of the tea stem, as shown in Figure 10. Click on Solve and once solved, the process of cutting the tea stalks is shown in Figure 11 to evaluate the maximum equivalent elastic strain of the model and the maximum force reaction of the two bionic cutting teeth.

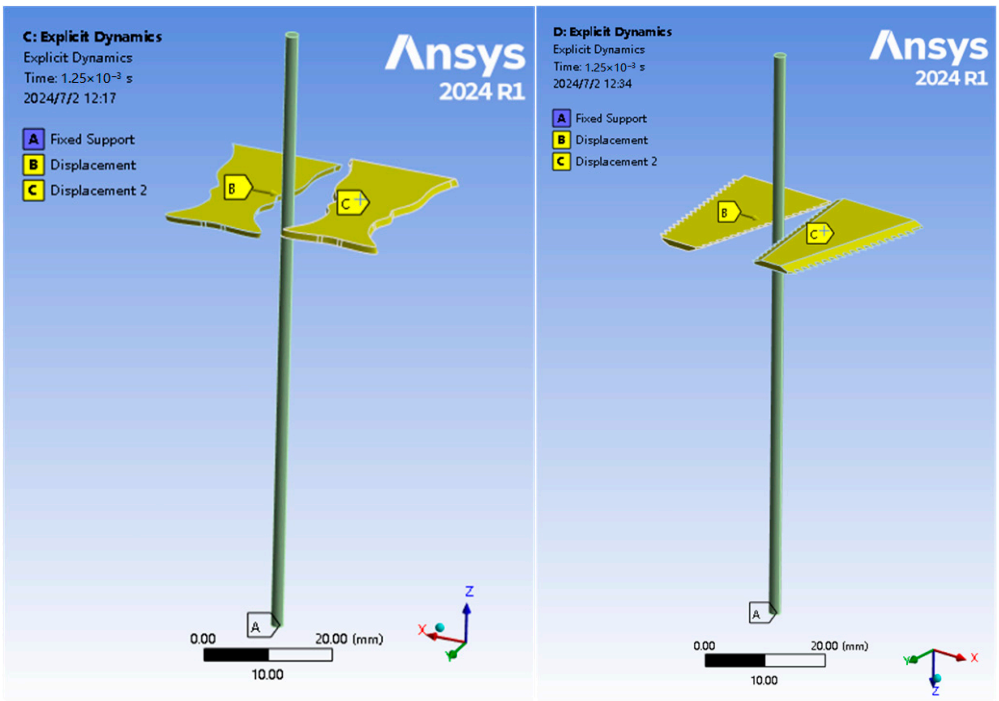


Figure 10. Explicit dynamics constraint load settings for bionic cutting teeth 3 and 4.

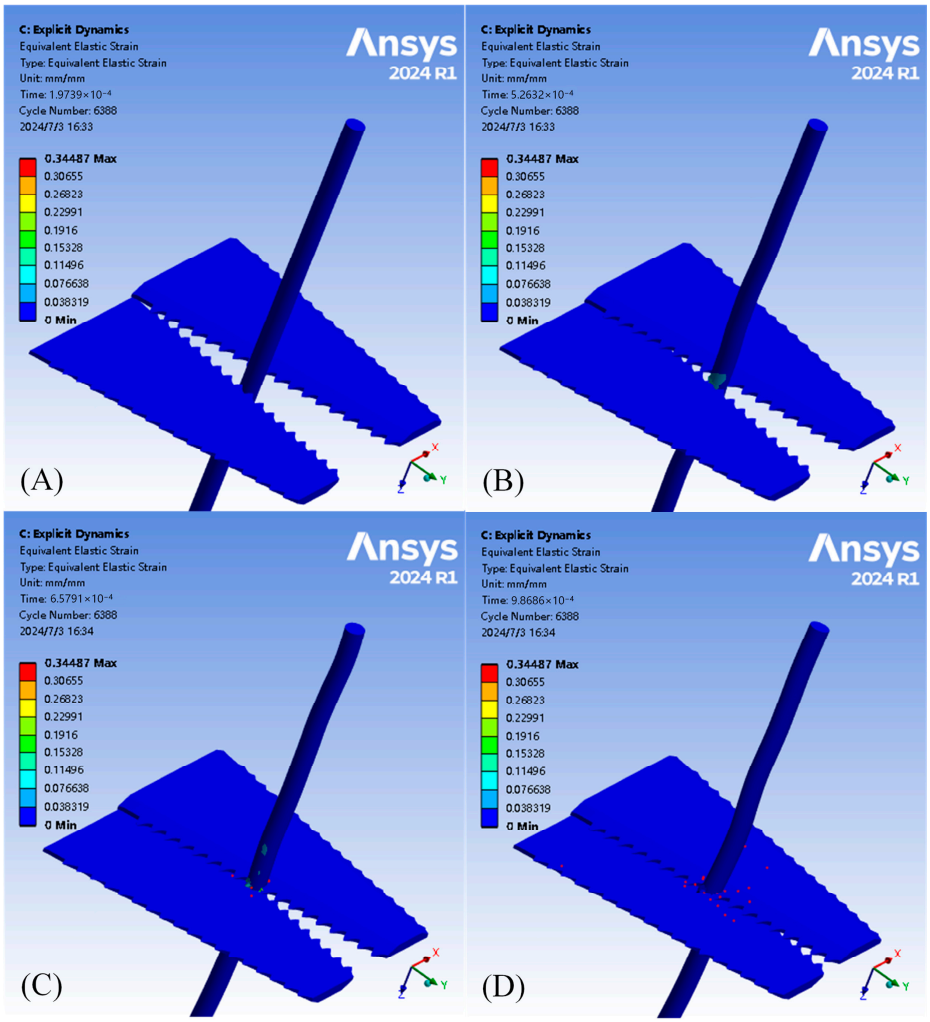


Figure 11. The cutting tea stalk process of bionic cutting teeth 3. (**A**) Before the cut, (**B**) Cutting starts, (**C**) Halfway cut and (**D**) Total cut.

The state of tea stalks and bionic cutting teeth before cutting is shown in Figure 11A. When the bionic cutting teeth start cutting, extrusion deformation occurs between the tea stalk and the cutting teeth edge surface. Subsequently, the bionic cutting teeth edges continue to move to squeeze the surface of the tea stem, and the surface of the stem begins to break, as shown in Figure 11B. When the bionic cutting teeth edges cut into the tea stalk at a certain depth, the surface of the tea stalk fracture is extruded with the beveled surface of the teeth edges, as shown in Figure 11C. Finally, the state when the tea stalk breaks and completely separates is shown in Figure 11D.

In this study, the relative cutting styles of ordinary trapezoidal teeth (Figure 12A), ordinary saw teeth (Figure 12F), and three bionic cutting teeth (as shown in Figure 12B–E,G) were compared one by one. Figure 12 shows the equivalent elastic strain cloud map of the explicit dynamic simulation test of ordinary trapezoidal teeth, ordinary saw tooth and three kinds of bionic cutting teeth. The red part is the part with large equivalent elastic strain, which can be clearly seen as the tangent position of the cutting teeth in the tea stalk, that is, the fracture site of the tea stalk.

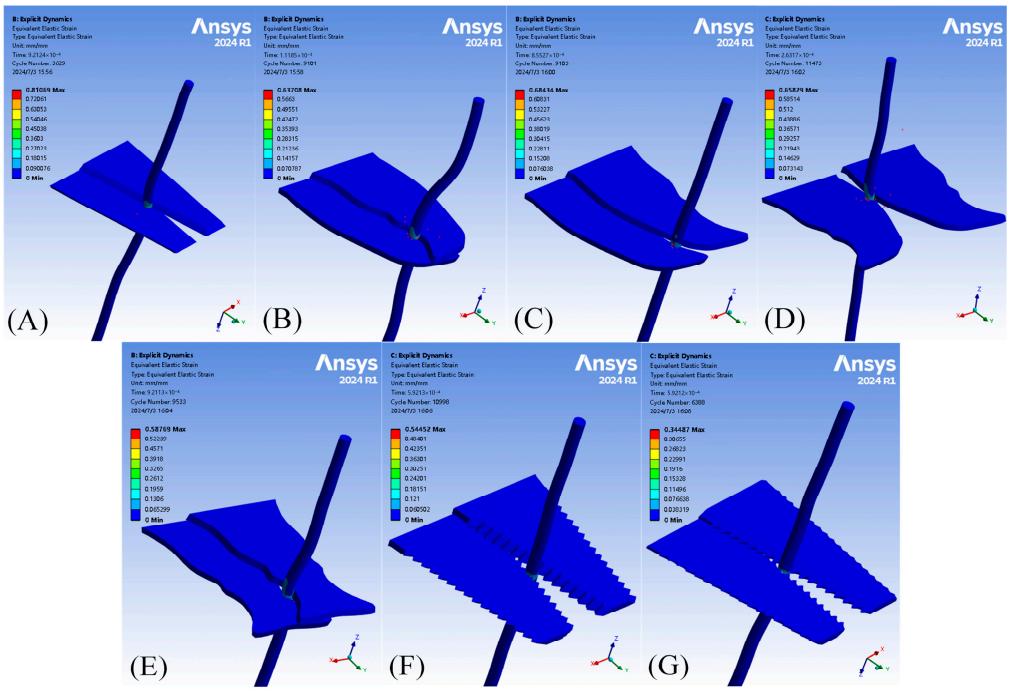


Figure 12. Explicit dynamic simulation test of 7 cutting collocation modes with 5 cutting teeth. (**A**) Cutting collocation mode of ordinary trapezoidal teeth; (**B**) Cutting collocation mode I of bionic cutting teeth l; (**C**) Cutting collocation mode II of bionic cutting teeth l; (**D**) Cutting collocation mode III of bionic cutting teeth l; (**E**) Cutting collocation mode of bionic cutting teeth 2; (**F**) Cutting collocation mode of ordinary saw teeth; (**G**) Cutting collocation mode of cutting teeth 3.

The data results of the equivalent elastic strain and force reaction data of tea stalks when cut by various cutting teeth are shown in Table 4, where force reaction is the maximum resistance generated by the movement of two cutting teeth of the same type, thus classified as left and right cutting teeth.

Table 4. Explicit dynamic simulation data results.

Cutting Teeth Relative Cutting Mode	Maximum Equivalent Elastic Strain	Maximum Force Reaction of the Left Cutting Tooth/N	Maximum Force Reaction of the Right Cutting Tooth/N
Ordinary trapezoidal teeth	0.811	13.266	15.702
Cutting collocation mode I of bionic cutting teeth l	0.637	13.1	12.532
Cutting collocation mode II of bionic cutting teeth l	0.684	14.632	14.195
Cutting collocation mode III of bionic cutting teeth l	0.658	14.14	13.694
Bionic cutting teeth 2	0.588	14.138	14.496
Ordinary saw teeth	0.545	10.734	10.033
Bionic cutting teeth 3	0.345	8.968	7.883

From Table 4, it can be seen that relative to the maximum equivalent elastic strain value of normal trapezoidal teeth, the three cutting pairings of bionic cutting teeth 1, bionic cutting teeth 2 and bionic cutting teeth 3 are reduced by 21.45%, 15.66%, 18.87%, 27.50% and 57.46%, respectively. It is obvious that the maximum equivalent elastic strain value of bionic cutting teeth 3 is much lower than that of ordinary trapezoidal teeth, bionic cutting teeth 1 and bionic cutting teeth 2. Compared with the maximum equivalent elastic strain value of the ordinary saw teeth, the bionic cutting teeth 3 is reduced by 36.70%.

Cutting resistance is an important index to judge the cutting performance of the cutter. Compared with the maximum force reaction value of ordinary trapezoid teeth, the three

cutting collocation modes of bionic cutting teeth 1, bionic cutting teeth 2 and bionic cutting teeth 3 decreased by 2.602 N, 1.070 N, 1.562 N, 1.206 N and 6.734 N, respectively. It is obvious that the maximum cutting resistance of bionic cutting teeth 3 is lower than that of ordinary trapezoidal teeth, bionic cutting teeth 1 and bionic cutting teeth 2. Compared with the maximum force reaction value of ordinary saw teeth, the bionic cutting teeth 3 is reduced by 1.766 N.

In summary, the maximum force reaction generated by the cutting collocation mode I (Figure 12B), mode II (Figure 12C) and mode III (Figure 12D) of bionic cutting tooth 1 is relatively large. Therefore, the cutting effect of bionic tea-harvesting cutter #3, represented by bionic cutting teeth 2 (Figure 12E), and #4, represented by bionic cutting teeth 3 (Figure 12G), are obviously better than those of bionic tea-harvesting cutters #1 and #2, represented by the three cutting collocations. And the maximum cutting force of the bionic cutting teeth 3 were smaller than that of the bionic cutting teeth 2 and the ordinary saw teeth. It is proved that bionic tea-harvesting cutter #4 requires the least cutting force in the operation of cutting and harvesting tea.

Furthermore, the bionic cutting teeth 3 (Figure 12G) produced the lowest maximum equivalent elastic strain value when cutting the stalks, which proved that the plastic deformation of the cutting surface of the tea stalk cut by the bionic tea-harvesting cutter #4, represented by the bionic cutting teeth 3, was the smallest, that is, the cut surface of the tea stalks was flatter when the operation was carried out with the bionic tea-harvesting cutter #4, which had the best effect and quality of the cut stalks. Therefore, it is more appropriate to choose the best bionic tea-harvesting cutter (#4) as the cutter of the tea stalk cutting device.

4. Discussion

Aiming at the main problems in the harvesting process of tea stalks, including high cutting resistance, high root damage and uneven cutting surface, this study carried out parameter optimization and bionic design of the reciprocating cutter of a hand-held portable tea picker, which provides important theoretical references to optimize the performance of the tea picker and to improve the cutting type end-effector. The main conclusions are as follows.

1. In this study, after an in-depth study of the microstructure of the upper jaw of the mouthparts of the *Aeolesthes induta* Newman based on the principle of bionics, the contour curve of the upper jaw of the mouthparts of the *Aeolesthes induta* Newman was extracted and optimized by using MATLAB, and the resulting curve data were applied to the cutting tooth of the reciprocating tea-harvesting cutter to design a set of new tea-harvesting cutters imitating the teeth of the *Aeolesthes induta* Newman, which contain four bionic tea-harvesting cutter schemes.
2. The key structural parameters of the bionic tea-harvesting cutter were determined, and the kinematic, static and dynamic models of the bionic tea-harvesting cutter, the bionic cutting tooth and the tea stalk were established in this study. In the kinematic simulation test, the results show that since curve 1 of the bionic tea-harvesting cutter #3 makes cutting times in a single cutting cycle than the first two bionic schemes, it better highlights its reliance on the bionically optimized design of the cutting teeth edge contour structure by mimicking the incisor lobe of the *Aeolesthes induta* Newman to carry out the cutting operation. Similarly, bionic tea-harvesting cutter #4 also highlights such advantages.
3. In the static simulation test, the results show that, relative to the maximum equivalent force value, equivalent elastic strain value and total deformation of the ordinary trapezoidal tooth, the values and deformation of bionic cutting tooth 3 of the bionic tea-harvesting cutter #4 are reduced by 81.83%, 82.01% and 44.88%, respectively, which are much lower than that of the ordinary trapezoidal teeth and are also lower than that of the bionic cutting tooth 1 and bionic cutting tooth 2. In addition, compared with the maximum equivalent stress value, equivalent elastic strain value and

total deformation of ordinary saw tooth, the bionic cutting tooth 3 is reduced by 29.54%, 29.23% and 6.80%, which proves that the bionic tea-harvesting cutter #4 represented by the bionic cutting tooth 3 has the best deformation resistance in the actual cutting process.

4. In the explicit dynamic simulation test, the results show that compared with the maximum equivalent elastic strain value and force reaction of the ordinary trapezoidal teeth, the bionic cutting teeth 3 of the bionic tea-harvesting cutter #4 are reduced by 57.46% and 42.89%, respectively, which is lower than the ordinary trapezoidal teeth, the bionic cutting teeth 1 and the bionic cutting teeth 2. In addition, compared with the maximum equivalent elastic strain value and force reaction of ordinary saw teeth, the bionic cutting teeth 3 decreases by 36.70% and 11.25%, which proves that the bionic cutting teeth 3 of the bionic tea-harvesting cutter #4 designed by this research team has the smallest plastic deformation in the actual cutting process. Compared with the traditional tea cutting tool, the bionic tea-harvesting cutter #4 cuts the tea stalk more smoothly, and the cutting effect and quality are the best.

5. Conclusions

In the field of agricultural harvesting, the bionic concept of "learning from nature and feeding back to nature" has certainly helped to promote the automation of various harvesting tasks in agriculture. This can not only alleviate the problems of labor shortage and substantial increase in harvesting costs brought about by an aging population and urbanization but also effectively reduces the cutting resistance of target agricultural products and the damage rate of crop stalks. In this study, the bionic tea-harvesting cutters designed can have excellent performance in the tea garden when harvesting and cutting tea, and its advantages of anti-deformation can reduce wear and damage and extend its service life. Secondly, the advantages of low resistance and high cutting quality of bionic cutting tools improve the quality and efficiency of tea picking and harvesting so as to further improve the quality of tea in the tea industry and reduce the economic losses after tea harvests. In addition, bionic tea-harvesting cutters or bionic cutting teeth can be installed on the end effectors of various tea picking machines or agricultural picking robots to carry out harvesting operations. However, there are some limitations in this paper. This study is only at the level of simulation on the bionic tea-harvesting cutter and bionic cutting tooth for comparison experiments, while future research on the basis of further optimization of the design of the bionic tea-harvesting cutter and bionic cutting tooth, as well as real-time control of the cutting speed of the tool according to the actual conditions of tea plantation cutting speeds, feed rates and cutting modes and other influencing factors will be experimented to further improve the advantages of the bionic technology in the field of agricultural harvesting.

Author Contributions: Data curation, Y.L., J.L. and S.H.; funding acquisition, Y.L. and W.W.; project administration, W.W.; formal analysis, Y.L. and J.L.; investigation, Y.L., J.L. and W.W.; methodology, Y.L., J.L., S.H. and W.W.; software, Y.L., J.L. and S.H.; supervision, Y.L., J.L., S.H. and W.W.; resources, Y.L., J.L. and W.W.; validation, Y.L., J.L. and W.W.; writing—original draft, Y.L., J.L. and W.W.; writing—review and editing, Y.L., J.L. and W.W. All authors have read and agreed to the published version of the manuscript.

Funding: This work was funded by the 2024 Rural Revitalization Strategy Special Funds Provincial Project (2023LZ04) and the Guangdong Province (Shenzhen) Digital and Intelligent Agricultural Service Industrial Park (FNXM012022020-1).

Institutional Review Board Statement: Not applicable.

Informed Consent Statement: Not applicable.

Data Availability Statement: The original contributions presented in the study are included in the article, further inquiries can be directed to the corresponding author.

Acknowledgments: The authors acknowledge the editors and reviewers for their constructive comments and all the support for this work.

Conflicts of Interest: The authors declare that we have no known competing financial interests or personal relationships that could have appeared to influence the work reported in this paper.

References

1. Li, J.; Li, J.; Zhao, X.; Su, X.; Wu, W. Lightweight detection networks for tea bud on complex agricultural environment via improved YOLO v4. *Comput. Electron. Agric.* **2023**, *211*, 107955. [CrossRef]
2. Zhang, Z.; Zhu, L.; Lin, G.; Zhang, S.; Guan, J. Research Progress on Key Technologies of the Famous Tea Picking End Effectors. *Mod. Agric. Equip.* **2022**, *43*, 7–12.
3. Nie, Y.; Chen, Y. Measurement of new shoot parameters and mechanical property analysis of plucking fingers for high-quality green tea. *Manuf. Autom.* **2022**, *44*, 83–86.
4. Liu, J.; Pan, Z.; Chen, Y.; Xiao, H.; Han, Y.; Hao, M. Development of the pneumatic control system for the bionic plucking fingers for high-quality green tea. *J. Chin. Agric. Mech.* **2021**, *42*, 166–170+188.
5. Hao, M.; Chen, Y.; Pan, Z.; Sun, Y. Development of a bionic plucking finger for high-quality green tea. *Food Mach.* **2018**, *34*, 86–90.
6. Wanieck, K.; Fayemi, P.E.; Maranzana, N.; Zollfrank, C.; Jacobs, S. Biomimetics and its tools. *Bioinspired Biomim. Nanobiomaterials* **2017**, *6*, 53–66. [CrossRef]
7. Lepora, N.F.; Verschure, P.; Prescott, T.J. The state of the art in biomimetics. *Bioinspiration Biomim.* **2013**, *8*, 013001. [CrossRef]
8. Bar-Cohen, Y. Biomimetics-using nature to inspire human innovation. *Bioinspiration Biomim.* **2006**, *1*, P1–P12. [CrossRef]
9. Luo, Y.; Li, J.; Yao, B.; Luo, Q.; Zhu, Z.; Wu, W. Research progress and development trend of bionic harvesting technology. *Comput. Electron. Agric.* **2024**, *222*, 109013. [CrossRef]
10. Sun, J.; Chen, H.; Wang, Z.; Ou, Z.; Yang, Z.; Duan, J. Study on plowing performance of EDEM low-resistance animal bionic device based on red soil. *Soil Tillage Res.* **2020**, *196*, 104336. [CrossRef]
11. Jia, H.; Li, C.; Zhang, Z.; Wang, G. Design of bionic saw blade for corn stalk cutting. *J. Bionic Eng.* **2013**, *10*, 497–505. [CrossRef]
12. Ren, L.; Han, Z.; Li, J.; Wang, J.; Tong, J. Experimental investigation of bionic rough curved soil cutting blade surface to reduce soil adhesion and friction. *Soil Tillage Res.* **2006**, *85*, 1–12. [CrossRef]
13. Tian, K.; Li, X.; Shen, C.; Zhang, B.; Huang, J.; Wang, J.; Zhou, Y. Design and test of cutting blade of cannabis harvester based on longicorn bionic principle. *Trans. Chin. Soc. Agric. Eng.* **2017**, *33*, 56–61.
14. Tian, K.; Zhang, B.; Shen, C.; Liu, H.; Huang, J.; Ji, A. Dynamic Cutting Performance Test and Parameter Optimization of Longicorn Bionic Blade for Industrial Hemp Harvester. *Agriculture* **2023**, *13*, 1074. [CrossRef]
15. Tian, K.; Li, X.; Zhang, B.; Chen, Q.; Shen, C.; Huang, J. Design and test research on cutting blade of corn harvester based on bionic principle. *Appl. Bionics Biomech.* **2017**, *2017*, 6953786. [CrossRef]
16. Tang, H.; Jiang, Y.; Wang, J.; Guan, R.; Zhou, W. Bionic design and parameter optimization of rotating and fixed stem-and leaf-cutting devices for carrot combine harvesters. *Math. Probl. Eng.* **2021**, *2021*, 8873965. [CrossRef]
17. Liu, Z.; Wang, T.; Liu, S.; Yan, X.; Zhao, H.; Wu, X.; Zhang, S. Design and experimental study of a bionic blade for harvesting the wild chrysanthemum stem. *Agriculture* **2023**, *13*, 190. [CrossRef]
18. Wu, C.C. Developing situation of tea harvesting machines in Taiwan. *Eng. Technol. Appl. Sci. Res.* **2015**, *5*, 871–875. [CrossRef]
19. Han, Y.; Xiao, R.; Song, Y.; Ding, Q. Design and evaluation of tea-plucking machine for improving quality of tea. *Appl. Eng. Agric.* **2019**, *35*, 979–986. [CrossRef]
20. Johnson, P.C.; Clementson, C.L.; Mathanker, S.K.; Grift, T.E.; Hansen, A.C. Cutting energy characteristics of Miscanthus x giganteus stems with varying oblique angle and cutting speed. *Biosyst. Eng.* **2012**, *112*, 42–48. [CrossRef]
21. Huang, M.; Li, Y.; Chen, A.; Xu, L. Design and test of double-cutterbar structure on wide header for main crop rice harvesting. *Appl. Sci.* **2020**, *10*, 4432. [CrossRef]
22. Han, Y.; Xiao, H.; Qin, G.; Song, Z.; Ding, W.; Mei, S. Studies on develop situations of tea-leaf picker both at home and abroad. *J. Chin. Agric. Mech.* **2014**, *35*, 20–24.
23. Su, N.; Chen, Q.; Zhang, Y.; Liu, W.; Li, C.; Liao, Z.; Huang, S. Population dynamics, spatial distribution pattern, mating and spawning behavior of Fenghuang Dancong tea tree longhorn beetle in Chaozhou. *J. Chin. Agric. Mech.* **2022**, *53*, 364–371.

Disclaimer/Publisher's Note: The statements, opinions and data contained in all publications are solely those of the individual author(s) and contributor(s) and not of MDPI and/or the editor(s). MDPI and/or the editor(s) disclaim responsibility for any injury to people or property resulting from any ideas, methods, instructions or products referred to in the content.